ISSN 0001-4338, Izvestiya, Atmospheric and Oceanic Physics, 2009, Vol. 45, No. 5, pp. 583–597. © Pleiades Publishing, Ltd., 2009.
Original Russian Text © V.G. Polnikov, 2009, published in Izvestiya AN. Fizika Atmosfery i Okeana, 2009, Vol. 45, No. 5, pp. 625–640.

A Comparative Analysis of Atmospheric Dynamic Near-Water Layer Models

V. G. Polnikov

A. M. Oboukhov Institute of Atmospheric Physics, Russian Academy of Sciences, Pyzhevskii per. 3, Moscow, 109017 Russia
e-mail: polnikov@mail.ru

Received May 22, 2008; in final form, September 12, 2008

Abstract—This paper considers the currently available approaches to constructing numerical models describing the dependence of parameters of the atmospheric near-water layer on heaving parameters (dynamic near-water layer). The models proposed in [1, 2] are characterized by detailed numerical algorithms, numerical calculations, and comparisons of the resistance coefficient C_d as functions of the parameters of the heaving surface, the state of which is given by the model two-dimensional wave spectrum as represented in [3]. For the same spectrum, the calculation results obtained by different models are shown to yield estimates for the value of C_d with a more than twofold discrepancy; however, the trends in the dependence of C_d on wave age and wind strength are close to one another and to observational data. Possible shortcomings of both approaches are analyzed, and ways to eliminate them are proposed. The requirements for setting special experiments needed to verify theoretical models of the dynamic near-water layer are discussed.

DOI: 10.1134/S0001433809050065

1. INTRODUCTION

Hereafter, when we refer to the atmospheric dynamic near-water layer (ADNWL) model, we will mean a system of equations allowing the characteristics of the atmospheric near-water layer to be calculated on the basis of the heaving state. Here, the characteristic variables of the near-water layer are the friction velocity u_* and the mean wind profile $\mathbf{U}(z)$, as well as the variables that are actually related to them (momentum flux to the boundary of media partitioning τ, wind velocity at the standard level $U(z)$, the friction coefficient $C_d(z) = u_*^2/U^2(z)$ related to the latter, etc.). On the other hand, the state of the stochastic field of heaving is most completely described by the two-dimensional spatial distribution of wave energy $S(k_x, k_y)$, where k_x and k_y are the components of wave energy vector $\mathbf{k}$ given in the space of wave numbers [4]. However, hereafter, we will use the representation $S(\mathbf{k})$ given by the frequency-angle spectrum $S(\omega, \theta)$ more often. Due to the unique dispersion relation between the frequency and wave vector $\omega(\mathbf{k})$, both representations of the field are physically equivalent. These characteristics of the system are implied to be linked to a certain spatial point $\mathbf{x}$ and time t with a given spectrum. Because the wave spectrum is a function of the wind field, a dynamic feedback between the wave and near-water characteristics appears which is reflected in the above-mentioned naming of ADNWL.

Building a physically sound model of the near-water layer that reasonably describes the existing large body of observational data is highly significant both theoretically and practically. Theoretically it is important due to the need to construct the most physically sound pattern of the relationship between the wind and wave. The practical importance is due to the problem of increasing the accuracy of the forecast of wave-heaving, as well as the general circulation of the atmosphere caused by more correctly specified boundary conditions at the underlying surface. It is clear that this is a very hard problem to be solved. Mostly, this is caused by the fact that the "atmospheric near-water layer–oceanic upper layer" includes flux and wave, as well as and turbulent, motions with highly differing characteristic timescales simultaneously. Because of this multiscale feature, the system cannot be described accurately and one has to use different hypotheses and simplifications typical for stochastic theories.

The problem under question can be solved with the help of three methods differing, in essence, by the level of physics and mathematics used.

The most comprehensive way is the approach using a numerical solution of the combined system of hydrodynamic equations describing the dynamics of all the elements of the boundary of media partitioning (some references can be found in [5]). Here, one can take into account the motions of all scales and use a minimum number of physical simplifications, which makes it possible to obtain the most accurate dependences required. However, this finding (i) involves the incontrollable consequences of the above-mentioned simplifications (especially related to the effects of instability of the wave profile) and (ii) it can be repre-

sented only numerically, which makes its physical interpretation particularly difficult. In addition, this approach is extremely labor-intensive to be widely applied, including in a comparison with experiments.

Another extreme case is the development and use of bulk-formulas that are rather simple analytical expressions linking together the heaving and near-water parameters (see, for example, [6]). The shortcoming of this approach is that it is difficult to ensure that bulk-formulas are justified and universal. Their development and use can be considered as the final stage of a more comprehensive study (see, for example, [5]).

An intermediate case is the approach to constructing an ADNWL model that combines simplicity and quantitative accuracy. Among these are the models where the state of heaving is known (i.e., given by the spectrum $S(\omega, \theta)$), and the above-mentioned integral characteristics (u_*, $\mathbf{U}(z)$, C_d) are calculated using equations for the closure of statistical characteristics of the system. These can be called semiempirical models. This approach has the additional advantage of numerical simplicity and speed, as well as physical clarity, which makes it possible to firmly analyze and interpret the results.

It is the semiempirical ADNWL models that will be considered hereafter. To date there have been several models of this type proposed in the literature [7]. Which of these models is the most adequate? There is no single answer, but it is this question that is considered in our paper.

Section 2 describes the main definitions and (briefly) the most significant of existing semiempirical approaches for ADNWL models. Section 3 gives a detailed algorithm for the calculation of $u_* C_d$ (10) as a functional of the spectral wave form $S(\omega, \theta)$ and wind strength $U_{10} = U(10)$ for two models [1, 2] that are theoretically the most justified and of practical interest. Section 4 presents the results of model calculations, their intercomparisons, and comparisons with observational data. Finally, Section 5 analyzes the advantages and shortcomings of both approaches and proposes some ways to eliminate the latter. In addition, experimental conditions necessary for a clear-cut verification of theoretical ADNWL models are formulated.

2. THE MAIN THEORETICAL POSTULATES AND VARIANTS OF ADNWL MODELS

2.1. The Main Theoretical Postulates and Problems of Constructing an ADNWL Model

For terminological definiteness, we describe (following [1, 2]) the main theoretical postulates used hereafter in describing ADNWL models.

The wind field in the atmospheric near-water layer is represented as

$$\mathbf{W} = \mathbf{U} + \mathbf{u}', \tag{1}$$

where $\mathbf{U}(z)$ is the average wind field and $\mathbf{u}'$ is the fluctuation (stochastic) component. The roughness of the boundary of media partitioning creates resistance to wind. This results in a flux of horizontal momentum to the surface of the boundary of media partitioning, which is called the wind stress τ. Its value is given by the relation

$$\tau_{x,z} = -\rho_a \langle u'_x u'_z \rangle = \tau \tag{2}$$

(hereafter, the ? sign will be omitted and the stress will be assumed to be normalized to air density ρ_a). For stationary wind, the momentum flux τ is assumed to be constant with respect to the vertical coordinate z,

$$\tau = \text{const} \tag{3}$$

and is the largest parameter of ANWL. Another major parameter is often taken to be the so-called friction velocity u_*, defined by the relation

$$\tau \equiv u_*^2. \tag{4}$$

In the case of a solid surface of the media-partitioning boundary, the value of τ is completely controlled by turbulent fluctuations of the wind field in the ANWL. The corresponding values of the flux and friction velocity denoted as τ_{t0} and u_{*0}, respectively, characterize the rate of "near-wall" (or, "background") turbulent fluctuations of the wind field. For these fluctuations, it can be assumed that $\tau = \tau_{t0}$ and the average wind profile $U(z)$ varies logarithmically:

$$U(z) = \frac{u_*}{\kappa} \ln \frac{z}{z_0}, \tag{5}$$

where $\kappa \approx 0.4$ is von Karman's constant. The independent theoretical parameter z_0 (emerging in (5)), which is called the roughness height or parameter, is determined experimentally. It is well established empirically that dependence (5) is satisfied for $z > 30\dfrac{\nu}{u_*}$, where ν is the kinematic viscosity of air [8]. For an aerodynamically smooth and flat wall (when the height h of irregularities of the media-partitioning surface is smaller than the thickness of the viscous sublayer; i.e., $h < \nu/u_*$), the following relation holds:

$$z_{t0} = a_n \nu / u_{*t0} \text{ at } a_n \approx 0.1, \tag{6}$$

where $\nu \cong 0.15$ cm^2/s is the kinematic viscosity of air. This also can be called background (near-wall) roughness [1, 8].

Over the perturbed surface of media partitioning, the wind-velocity fluctuations have an additional wave component $\mathbf{u}'_w$, ; i.e., we have

$$\mathbf{u}' = \mathbf{u}'_t + \mathbf{u}'_w. \quad (7)$$

There is a definition for $\mathbf{u}'_w$ which will not be discussed here due to its unimportance (see [1] for details). It is merely important that the wind stress is split into turbulent τ and wave τ_t components. Here it would be justified to assume that the total flux is independent of the vertical coordinate z:

$$\tau \equiv u_*^2 = \tau_t + \tau_w = \text{const}. \quad (8)$$

In this case, τ_t is not necessarily identically equal to τ_{t0}; for τ_w, it is widely accepted that, at the zero level ($z = 0$) corresponding to the ensemble-mean wave boundary of media partitioning, the following relation is true:

$$\tau_w(z = 0) \equiv \tau_w(0) = \rho_w g \int \frac{k\cos(\theta)}{\omega} IN(S, \mathbf{U}, \omega, \theta) d\omega d\theta. \quad (9)$$

Here, ω and $k(\omega)$ are the frequency and wavenumber, respectively, of the wave-field component given by the energy frequency–angle spectrum $S(\omega, \theta)$; θ is the direction of wave-component propagation with respect to a specified direction; and $IN(\ldots)$ is the term of the source function of the spectral model of wave evolution, which is responsible for the rate of energy transfer from wind to waves (the so-called "pumping mechanism" term). See [1, 2] for details.

Hereafter, we suppose that the analytical representation of $IN(\ldots)$ is known and the wave component of the vertical flux of momentum to the boundary of media partitioning z is uniquely determined. Thus, if τ_w depends on z, the turbulent component satisfies the relation

$$\tau_t(z) = u_*^2 - \tau_w(z). \quad (10)$$

The aim of ADNWL theory is reduced to determining the values of the total momentum flux τ as well as to profiling the average wind $U(z)$ on the state of heaving. In this case, the wind profile $U(z)$ must be derived from closure equations of the ADNWL model. Generally, the form of the profile $U(z)$ will not necessarily coincide with standard logarithmic profile (5); rather, it will supplement (5), especially in the range of small values of z, where this formula cannot be used. In addition, in the physical sense, it is interesting to consider the vertical distribution of τ_t and τ_w, as well as a series of other accompanying problems which will not be detailed here.

It is this stage of the theory that is characterized by emerging differences in approaches to describing ADNWL. Among these, the following well-known variants can be mentioned:

(1) The turbulent component of stress is always invariant and constant with respect to z (i.e., $\tau_t = \tau_{t0}$), and all the remaining terms in τ constitute the wave component τ_w [1]. Here, the thin near-water layer where the fluxes $\tau_w(z)$ and $\tau_t(z)$ can be vertically changed is actually disregarded. Above this layer, a type-(5) logarithmic law of change is assumed for $U(z)$ where the parameter z_0 depends on the state of heaving (i.e., on the wave spectrum $S(\omega, \theta)$).

(2) The wave component τ_w of stress depends on z, bringing a z-dependence of the turbulent component into existence (in line with (10)). The latter fact leads to a separate equation for the wind velocity profile $U(z)$. As a result, all the dependences mentioned above can be calculated by certain analytical formulas (for example, [2, 9]).

(3) The average-wind profile $U(z)$ is always logarithmic, and, under heaving, τ_{t0} and $\tau_t(z)$ are calculated from (5) with the help of closure models for $\tau_t(z)$ [10].

Restricting ourselves by the references cited above, we will consider the given approaches in the chronological order of their appearance to select the most suitable (for applications) variants of ADNWL models.

2.2. ADNWL Model Based on Janssen's Study [10]

In all cases, the turbulent component of the momentum flux is calculated by the formula

$$\tau_t = l^2 \left|\frac{\partial U(z)}{\partial z}\right| \frac{\partial U(z)}{\partial z}, \quad (11)$$

where the mixing length l is assumed to be proportional to the distance to the mean surface: $l = \kappa z$. The wind profile satisfies the logarithmic law of (5) if there are no waves, and it has the following rather specific form when heaving is present:

$$U(z) = \frac{u_*}{\kappa} \ln \frac{z + z_w}{z_0 + z_w}. \quad (12)$$

In [10], the "background" value of z_0 is calculated from Charnock's relation $z_0 = \alpha_{ch} u_*^2 / g$ for certain values of the parameter α_{ch} on the order of $\cong 0.01$. The additional variable z_w – is merely the required additive wave-induced component; however, $U(z_0) = 0$ (here, the notations of [10] are used). According to [11], the turbulent component of stress is known and can be given analytically as

$$\tau_t(z) = \tau \left(\frac{z}{z + z_w}\right)^2. \quad (13)$$

The wave component τ_w of momentum flux is given by relation (9), where $IN(\ldots)$ can be conve-

niently expressed as a product of dimensionless multipliers and the dimensional quantity $\omega S(\omega, \theta)$:

$$IN(\ldots) = \left\{\frac{\rho_a}{\rho_w}\left(\frac{u_*}{\omega/k}\right)^2\beta(u_*, \omega, \theta)\right\}\omega S(\omega, \theta). \quad (14)$$

In [10], the value of the increment $\beta(u_*, \omega, \theta)$ is parameterized according to author's own calculations by the Miles model of wave generation by wind [11] using the formula

$$\beta = \left[\frac{1.2}{\kappa^2}\mu\ln^4\mu\right]\cos^2(\theta - \theta_w) \quad (\text{at } \mu \le 1). \quad (15)$$

Here, $\mu = k(z_w + z_c)$ is a theoretical parameter zeroing the increment β for a particular value of the module of wavenumber k, which is quite important for integral (9), which determines τ_w, to be finite.

In this approach, the dependence $\tau_w(z)$ is not considered because the value of τ_t is taken from relation (13) at height $z = z_0$. In this case, the value of z_w is calculated through the ratio of components of the complete flux of momentum, which, together with (10) and (13), yields

$$z_w = z_0[(1 - \chi)^{-1/2} - 1]. \quad (16)$$

Finally, the complete flux of momentum τ at the level z is calculated from the transcendent equation (17)

$$\tau = \left\{\frac{\kappa U(z)}{\ln[z/(z_0 + z_w)]}\right\}^2 \quad (18)$$

by the method of iterations.

This approach has the advantage of the theoretical result of (15), according to which τ_w is always calculated at a finite of interval of frequencies. However, having been obtained by the numerical solution of the Miles problem formulated in the potential approximation, (15) it is not indisputable. In addition, the hypothetic elements of this approach are both formulas (11) and (12) and whether the logarithmic resistance law is applicable up to the level of mixing height (and, consequently, relations (13), (16), and (17)). Because of this, we will not numerically analyze Janssen's approach.

2.2. ADNWL Model Based on Zaslavski's Studies [1, 7, 12]

The most significant feature of this approach is that it is based on a number of nonstandard assumptions that are described below in separate items.

2.2.1. The turbulent component of stress τ_t is assumed to be independent of the state of heaving (i.e., always invariant):

$$\tau_t = \tau_{t0}. \quad (19)$$

This flux corresponds to the quite definite "near-wall" friction velocity

$$u_{*t0} = (\tau_{t0})^{1/2}. \quad (20)$$

This velocity can be found by using the Kazanski–Monin resistance law [11] for the atmospheric planetary boundary layer (APBL) given by the exact theoretical formula

$$u_{*t0} = \kappa U_g\left[\left(\ln\frac{u_{*t0}}{fz_0} - B\right)^2 + C^2\right]^{-1/2}. \quad (21)$$

Here, U_g is the local geostrophic wind on the upper boundary of the APBL, f is the Coriolis parameter, Ω is the angular velocity of the Earth's rotation, and φ is the local latitude. According to Zaslavski, z_0 in Eq. (20) is the sea-surface roughness height when no waves are present. The values of constants A and B depend on the APBL stratification and are assumed to be known.[1]

2.2.2. The value of z_0 is assumed to be determined by the standard relation of the theory of near-wall turbulence (6). In this formulation, the joint solution of system (6) and (20) uniquely estimates both u_{*t0} and z_{t0} for fixed values of all the remaining system parameters.

2.2.3. In case of waves, the same theoretical relations (8) and (9), as well as law (20), are used, resulting in two independent equations

$$u_*^2 = u_{*t0}^2(U_g, f, \nu, A, B) + \tau_w(u_*, S)/\rho_a \quad (22)$$

and

$$u_* = \kappa U_g\left[\left(\ln\frac{u_*}{fz_w}B\right)^2 + C^2\right]^{-1/2}, \quad (23)$$

making it possible to determine both the total friction velocity u_* and total roughness height z_w when waves are present (which is then used in formula (5) for the wind profile)). The value of the eave component of the momentum flux τ_w in (21) is described by the commonly accepted relation (9) and assumed to be the additive component of the total flux, which is constant in the vertical.

To obtain a complete solution of the ADNWL problem, it is necessary to assess the average-wind profile. Zaslavski did not describe $U(z)$ up to $z = z_w$ in detail to set the wind profile by the standard logarithmic law (5) "outside the layer of momentum outflux to waves." In fact, this model disregards the portion of the APBL that does include the wave component of velocity fluctuations u_w'. This makes it possible to disregard the vertical distribution of the wave portion of

[1] The use of law (20) in the given ADNWL model was first published in [12], where the NWL parameters were calculated by I.M. Kubatchenko. This allows one to consider him a co-author of this model.

the momentum flux $\tau_w(z)$, taking it as the additive supplement to τ_{t0}. As a result, the entire layer that is characterized by the heaving influence on wave-flux fluctuations is not considered. Thus, the average wind profile is assumed to satisfy a type-(5) logarithmic law.

By the way, the latter proposition of Zaslavski's model (withdrawing the dependence $\tau_w(z)$) can be attributed to the faults of the theory, just like the use of the Coriolis parameter f, which depends on the local latitude. At the same time, it should be accepted that the idea of using friction law (20) in the ADNWL problem is a delicate move to avoid various types of closure hypotheses that are inevitable in this problem. Thus, in our study, we investigated this approach to use it as a reasonable alternative for constructing an ADNWL model.

2.3. ADNWL Model by Chalikov [9] and Makin–Kudryavtsev [2]

We believe that the theoretical proximity of the approaches proposed in a series of works by Chalikov and co-authors (see references in [9]) and finalized in a certain way (quite neatly) in [2] makes it possible to consider them combined. The main postulates in these works are as follows.

2.3.1. An analysis of the APBL variability scales makes it possible to state that relation (8) can be used at timescales that are below synoptic but an order of magnitude higher than the period of waves and outside the viscous sublayer ($z > z_0^{\nu} \equiv z_{0t}$, where z_{0t} is determined by relation (6)).

2.3.2. The turbulent component of wind stress τ_t is determined only by the average-wind profile $U(z)$ in the APBL. In this case, according to the classical theory of stress closure [8], these quantities are related as

$$\tau_t(z) = K\frac{\partial U(z)}{\partial z}, \tag{24}$$

where K is an unknown vertical exchange coefficient. To find this coefficient, the authors of [2, 9] use the equations of turbulent energy balance and a number of suppositions typical for the theory of turbulence, which allows K to be expressed through u_* and τ_t in some approximation (see the original papers). In this case, one can integrate (23) to obtain an analytical expression for the wind profile at heights located above the viscous sublayer ($z > z_0^{\nu}$):[2]

$$\begin{aligned} U(z) &= u_*^2\int_{z_0^{\nu}}^{z}\left[1-\frac{\tau_w(z)}{u_*^2}\right]K^{-1}dz \\ &= \frac{u_*}{\kappa}\int_{z_0^{\nu}}^{z}\left[1-\frac{\tau_w(z)}{u_*^2}\right]^{3/4}d(\ln z) \equiv \frac{u_*}{\kappa}F(z). \end{aligned} \tag{25}$$

As a result, for wind at a fixed (standard) height (for example, $U(10) \equiv U_{10}$), the value of u_* is completely controlled by the state of heaving.

2.3.3. Now, the problem is reduced to finding the distribution of the wave component of stress by the vertical $\tau_w(z)$. In this issue, the approaches of Chalikov and Makin–Kudryavtsev (MK) diverge. Chalikov tries to find this dependence using analytical techniques, while MK solves this problem numerically. Both variants are of an approximate character; however, in our opinion, the result of the MK approach is briefer and we use this approach for further calculations. Omitting the details of the transformation of MK-formulas into more convenient expressions, we give the expression for the final term $\tau_w(z)$, where only the authentic vertical structure for the wave component of momentum flux is retained:

$$\begin{aligned} t_w(z) = u_*^2\int_{\omega_{\min}}^{\omega_{\max}}\oint_{\theta}\tilde{u}_*^2[\exp(-10zk)\cos(5\pi zk)] \\ \times\beta(u_*,\omega,\theta)S(\omega,\theta)k^2\cos(\theta)d\sigma d\theta. \end{aligned} \tag{26}$$

Here, it is the expression in square brackets under the integral in (25) that is the vertical structure of function $f(z, k)$ of the wave component of momentum flux $\tau_w(z)$.[3]

2.3.4. The specific feature of the MK-approach, reflected by the presence of the auxiliary function $\tilde{u}_*^2$, under the integral in formula (25), is that, according to the authors of [2], the wave portion of the momentum is determined by the fact that only the turbulent component of fraction velocity (rather than the full velocity) is used in the pumping function IN. In this case, the expression for $\langle\tilde{u}_*^2\rangle$ takes the form

$$\tilde{u}_*^2 = 1 - \langle f(k)\rangle_z\frac{\tau_w(0)}{u_*^2}, \tag{27}$$

[2] Here, we note that the choice of the lower limit of integral (24) is open for discussion.

[3] Here, it makes sense to immediately note that the specific form of $f(z, k)$, which was taken without any changes from [2] and shown in (25), is not determined once and for all. In subsequent calculations, this form can be adjusted in terms of selecting constants and using an oscillating multiplier of the form $\cos(5\pi zk)$.

where

$$\langle f(k)\rangle_z = \int_0^\infty f(z)\exp(-z/\delta)d(z/\delta) \quad (27a)$$

$\delta \approx 0.01/k$ is the height of the internal interaction sublayer, and

$$f(z) = \frac{1}{\tau_w(0)}\int_{\omega_{\min}}^{\omega_{\max}}\oint_\theta[\exp(-10zk)\cos(5\pi zk)] \times \tilde{I}\{\beta, \omega, S(\omega, \theta)\}k^2\cos(\theta)d\omega d\theta \quad (27b)$$

(see [2] for details). Let us note that it is proposition 2.3.4 of the MK-model that can be most seriously criticized later (see below).

This completes the general description of approaches to the construction of ADNWL models, and we can turn to describing algorithms for the implementation of models 2 and 3.

3. CALCULATION ALGORITHMS FOR TWO ADNWL MODELS

3.1. General Elements of Algorithms

All ADNWL models include the general feature of using similar formulas for calculating the wave component of momentum flux (integrals (9) and (25)). This makes it necessary to specify a frequency–angle numerical grid $\{f_n, \theta_m\}$ (where, for convenience in the spectrum representation, one uses the cyclic frequency $f = \omega/2\pi$ specified in Hz) and the model form of the spectrum $S(f, \theta)$, which is reduced to the specification of the form of the supplement $\beta(u_*, \omega, \theta)$ (see formula (14)).

The choice of the frequency grid given by the following law typical for wave problems

$$f_n = f_0 e^n \text{ at } 0 \le i \le N, \quad (28)$$

is characterized by a minimum frequency f_0, the grid increment e, and the number of points in grid N. In our calculations, the value of e is equal to 1.05 and the number of points in the grid varies in the range between 100 and 120 to ensure an adequate frequency maximum $\omega_{\max}$ of around 80–100 r/s, which is sufficient for the corresponding integral to be correctly estimated.[4] The values of f_0 vary in the range between 0.4 and 0.16, depending on the value of U_{10}, in order to provide calculations of τ_w in a wide range of reverse wave ages $A1$, which are commonly used in analyzing empirical data and given by the relation

$$A1 = u_*\omega_p/g, \quad (29)$$

where ω_p is the peak of spectrum $S(\omega, \theta)$. Here, the variations in velocity U_{10} were considered in the range from 5 to 25 m/s, and the wave age was varied by setting the values of ω_p within the values of $A1$ from 0.01 to 0.1 typical for observational data [6, 14, 15].

In this problem, the grid with respect to angular variable $\{\theta_m\}$ is unimportant. For our purposes, a uniform distribution of $\{\theta_m\}$ with a step of $\Delta\theta = 10°$ is quite suitable.

The choice of the model spectrum is a key item in this study, because there are almost no reliable empirical data energy wave spectra at such a wide frequency range. This problem needs special investigations like [16], which are full of suppositions and far from being finalized due to lack of measurements. This fact made it inevitable to vary the spectrum forms known from experiments.

Because the main tendencies of the behavior of the dependences of $C_d(10)$ on wind velocity U_{10} and wave age are rather well-known [6, 14, 15] (namely, the variation range of $C_d(10)$ is bounded by the interval 0–0.003; $C_d(10)$ slowly grows with the growth of U_{10} and growth of back age $A1$), it is important to find similar dependences in calculations too. Based on the results of numerous tests, we decided to take the spectrum proposed in [3] as a basis. In our study, this spectrum is represented as

$$S(f, \theta) = D(A)\frac{2\pi g^2}{(2\pi f)^5}\frac{f}{f_p}\exp\{-1.25(f_p f)^4\} \times \exp\left\{\ln(\gamma(A))\exp\left[-\frac{(f-f_p)^2}{0.02f_p^2}\right]\right\}\Psi(f, \theta). \quad (30)$$

Here,

$$D(A) = 0.006/A^{0.55} \quad (31)$$

and

$$\gamma(A) = 1.7 - 6\log(A) \quad (32)$$

are unique multipliers introduced in [3] to describe the dependence of the heaving intensity and frequency narrowness of the spectrum on the wave age A given by the relation

$$A = g/(2\pi f_p U_{10}). \quad (33)$$

The remaining frequency multipliers have a form typical for the well-known spectrum JONSWAP [4], which means we don't have to describe it.

The angular function of spectrum $\Psi(f, \theta)$ was represented in the simplest commonly accepted way as

$$\Psi(f, \theta) = I_n\cos^n(\theta - \theta_u), \quad (34)$$

[4] The choice of $\omega_{\max}$ is of a heuristic character and controlled by conditions of the small variability of a finite value of the integral and by excluding capillary waves from consideration, which is conditioned by the applicability limits of formulas for the increment of growth of $\beta(u_*, \omega, \theta)$ and by the parametrization for the model wave spectrum.

where $I_n = (\oint \cos^n\theta\, d\theta)^{-1}$ is a normalizing multiplier and $\theta_u = 0$ is the model wind direction. In our calculations, the influence of the form of $\Psi(f, \theta)$ on estimates for ANWL parameters is essentially weaker than the influence of the frequency dependence on spectrum $S(f, \theta)$; therefore, we will present the results of calculations below only for the case of $n = 2$.

Another essential component of any ADNWL model is the choice of the increment of the pumping function $\beta(u_*, \omega, \theta)$. In our calculations, we used the expression

$$\beta = c_\beta\left\{[1 + 0.136\left(\frac{u_*\omega}{g}\right)^{-1} + 0.0137]\cos(\theta - \theta_u)\right. \\ \left. - 0.00775\left(\frac{u_*\omega}{g}\right)^{-2}\right\}, \quad (35)$$

where c_β is a dimensionless coefficient with values spanning the range between 30 and 60. The form of (35) is one of the representations of the generalized formula for $\beta(u_*, \omega, \theta)$ constructed in [17].[5] Its main advantage over many other analogs is that it can be applied to a very wide frequency range: $1 \le U_5\omega/g \le 75$, which is of key importance in terms of obtaining reliable estimates for integrals (9) and (25). At this stage of investigations, it is not yet of key importance to vary the form of the expression entering into the brackets of expression (35), but it quite reasonable to vary the constant c_β. However, this variation is bounded by certain limits discussed below. The main results of calculations are shown for $c_\beta = 45$.

Here, it should be noted that the law of fall-off for the high-frequency component of spectrum (30), which involves the range $f > 3f_p$, corresponds to the dependence f^{-4} (the so-called law of spectrum "tail" fall-off). However, it can be easily seen that the convergence of integrals (9) and (25) for spectra declining proportionally f^{-4} is quite problematic. One way to solve of this problem was to vary the form of (30) by eliminating the multiplier f/f_p from it and obtain the well-known law of Phillips fall-off $S(f) \propto f^{-5}$ [4]. Therefore, to provide more freedom to choose the most adequate ADNWL model, we had estimated the dependences of ANWL parameters on the state of heaving for both above-mentioned versions of the model spectrum, which, hereafter, will be conditionally denoted as S_{-4} and S_{-5}.

It is apparent that the final solution to the problem of integral convergence for the wave component of momentum flux (9) requires more accurate knowledge of both the behavior of spectrum $S(f, \theta)$ at high frequencies and the form of the increment of pumping function $\beta(u_*, \omega, \theta)$ in the integral. A number of aspects of this problem are discussed in detail in the final section of this paper.

3.2. Zaslavski's Model

Let us consider in more detail the ADNWL model by Zaslavski (see Section 2.2). To this end, we should describe the method of solving the system of equations of (6) and (21)–(23) controlling the ANWL dynamics with or without heaving.

For "background" values (i.e., without heaving), the solution of (6) and (21) is reduced to substituting expression (6) into equation (20). For given values of U_g, local latitude φ, and stratification parameters B and C, the final irrational equation of the form

$$u_{*t0}^2 = \frac{(\kappa U_g)^2}{(\ln[u_{*t0}^2/fa_n\nu] - B)^2 + C^2} \quad (36)$$

can be easily solved with respect to u_{*t0} by the interval bisection method. In this way, the turbulent component of momentum flux τ_{t0} and roughness z_{t0} become uniquely determined.[6]

When there is heaving given by the spectrum $S(f, \theta)$, using the wave pumping function IN, expressed in the most general form as

$$IN = c_\beta\frac{\rho_a}{\rho_w}\frac{u_*^2}{(g/\omega)^2}\beta(u_*\omega, g, \theta)\omega S(\omega, \theta), \quad (37)$$

the value of τ_w is calculated, which can be conveniently represented in terms of the dimensionless $\tilde{\tau}_w$, as

$$\tilde{\tau}_w(S) = c_\beta\iint\beta(\ldots)\cos(\theta)k^2S(\omega, \theta)d\omega d\theta. \quad (38)$$

Then, we have $\tau_w = u_*^2\,\tilde{\tau}_w$, and it immediately follows from equation (21) that the complete friction velocity can be expressed as

$$u_*^2 = \frac{\tau_{t0}}{1 - \tilde{\tau}_w(S)}. \quad (39)$$

By its order of magnitude, $\tilde{\tau}_w$ has the value of the average square of the wave-field steepness multiplied by c_β. Therefore, according (39), the structure of multiplier

[5] Here, similarly to formula (14), the standard formula for β is normalized to the multipliers ρ_a/ρ_w and $(u_*\omega/g)^2$, which are reduced when integrals (9) and (25) are calculated.

[6] The knowledge of these parameters makes it possible (with the help of (5)) to determine the height at which the wind velocity $U(z)$ becomes comparable with U_g, which of itself can be of certain interest (the dependence of APBL height on characteristics of the underlying surface.)

$\beta(u_*, \omega, \theta)$ must be so in order to guarantee the following inequality

$$\tilde{\tau}_w < 1. \quad (40)$$

Only in this case, the expression for the complete friction velocity u_* remains true and formula (39) uniquely ensures that u_* can be calculated for a heaving surface. Then, the value of the complete roughness height z_w is determined from relation (22):

$$z_w = \frac{u_*}{f\exp[(\kappa^2 U_g^2/u_*^2 - C^2)^{-1/2} + B]}, \quad (41)$$

and the wind profile is calculated by formula (5).

Finally, we note that the friction coefficient for all states of a rough-sea surface is determined by the standard relation

$$C_d(z) = u_*^2/U^2(z) \quad (42)$$

with the help of the corresponding values of friction velocity u_* and the roughness height required for determining $U(z)$.

3.3. The Makin–Kudryavtsev Model

The main uncertainties in this model are (a) the correction of the form of auxiliary function $\tilde{u}_*^2$, entering into the integral in (25), (b) the correction of the final expression for $U(z)$, and (c) the integration over the vertical direction in main formula (24).

The first question is solved by using the simplification

$$\langle f(k)\rangle_z \approx 1. \quad (43)$$

This approximation follows from a qualitative analysis of the set of formulas (27). In this case, expression (26) for $\tilde{u}_*^2$ is essentially simplified and the final expression for $U(z)$ takes the form

$$U(z) = \frac{u_*}{\kappa}\int_{z_0^v}^{z}\left[1 - \frac{J(z)}{1 + J(0)}\right]^{3/4} d(\ln z) = \frac{u_*}{\kappa}F(z), \quad (44)$$

where

$$J(z) = \int_{\omega_{\min}}^{\omega_{\max}}\oint_{\theta}[\exp(-10zk)\cos(5\pi zk)] \times k^2\beta(\ldots)S(\omega, \theta)\cos(\theta)d\omega d\theta. \quad (45)$$

The integration with respect to height z in (44) is performed on a grid given uniformly in the logarithmic coordinates $z' = \ln(z)$ in the range from $z = z_0^v = 5 \times 10^{-5}$ m to $z = 10$ m with the number of points $NZ = 21$.

This makes the calculation scheme by the Makin–Kudryavtsev model fully definite. For a given value of U_{10} and a form of spectrum $S(\omega, \theta)$, the set of values of the integral $J(z)$ is then used for calculating the integral $F(z)$ by formula (46). This yields the expression for complete friction velocity

$$u_* = \kappa U_{10}/F(10) \quad (46)$$

and the related variables (τ and $C_d(10)$). At all heights (in the above-mentioned range), the wind profile $U(z)$ is determined by using the same formula (44) and there is no need to introduce the roughness height (see [18] for a detailed discussion of these issues). If one wants to introduce an efficient ANWL parameter similar by its meaning to z_w [18], one can use a logarithmic wind profile like (5) to obtain

$$z_w = 10/\exp[\kappa U_{10}/u_*], \quad (47)$$

which is suitable for comparing the MK model with both experimental data and other ADNWL models.

It follows from the discussion in this section that, among the variants considered here, the MK model formally yields the most comprehensive solution of the ADNWL modeling problem. However, in the practical aspect, the final decision on the preference of a given model can be made only through special testing and verification (i.e., by comparison with experimental data). The first part of such a study is presented in the next section.

At present, a comprehensive verification of models seems to be impossible because of lack of data on the synchronous measurements of the form of wave spectrum $S(f, \theta)$ and ANWL parameters. Its weak analog was constructed by using measurement data taken from [15]. A detailed discussion of verification problems can be found in the final section of this paper.

4. RESULTS OF TEST CALCULATIONS AND THEIR ANALYSIS

4.1. Zaslavski's Model [12]

For the values of model parameters $B = 3.1 - 0.1\,U_g$ and $C = 4.4$ (close to the empirical values of B and C in [19]), the calculation results for the latitude $\varphi = 45°$ and a (30)-type spectrum are presented in Tables 1 and 2 for two values of geostrophic wind U_g.

Analyzing the whole set of calculations with Zaslavski's model for the spectrum S_{-4}, we can conclude the following (see Tables 1 and 2):

4.1.1. The background value of the friction coefficient C_{10t0} slowly decreases with a rise in velocity on the upper boundary of the APBL given by the value of U_g. Here, the ratio of background velocity at the level of 10 m to U_{10t0} has the same trend.

4.1.2. As the wave age grows (accompanied by a decrease in the frequency of the peak of spectrum U_g),

Table 1. Results of calculations with Zaslavski's model for the wind U_g = 10 m/s and spectrum S_{-4}

U_g, m/s	U_{10t0}, m/s	U_{10w}, m/s	C_{10t0}, 10^{-3}	C_{10w}, 10^{-3}	A, 10^{-1}	$A1$, 10^{-2}	f_p, Hz
10	7.88	7.15	7.93	1.47	3.68	10.4	.594
		7.10		1.53	3.83	10.2	.574
		7.05		1.59	4.00	9.97	.554
		7.0		1.65	4.18	9.73	.534
		6.94		1.72	4.37	9.48	.514
		6.89		1.79	4.59	9.22	.494
		6.84		1.86	4.82	8.95	.474
		6.73		2.01	5.11	8.78	.454
		6.68		2.09	5.38	8.49	.434
		6.57		2.26	5.74	8.28	.414
		6.46		2.44	6.13	8.05	.394
		6.36		2.63	6.57	7.81	.374
		6.24		2.84	7.06	7.55	.354
		6.08		3.19	7.69	7.35	.334
		5.91		3.59	8.42	7.12	.314

Table 2. Results of calculations with Zaslavski's model for the wind U_g = 25 m/s and spectrum S_{-4}

U_g, m/s	U_{10t0}, m/s	U_{10w}, m/s	C_{10t0}, 10^{-3}	C_{10w}, 10^{-3}	A, 10^{-1}	$A1$, 10^{-2}	f_p, Hz
25	17.8	15.7	7.14	1.41	2.28	16.5	.437
		15.6		1.44	2.40	15.8	.417
		15.5		1.50	2.54	15.3	.397
		15.2		1.61	2.71	14.8	.377
		15.1		1.68	2.89	14.2	.357
		14.9		1.79	3.11	13.6	.337
		14.6		1.91	3.36	13.0	.317
		14.3		2.14	3.68	12.6	.297
		13.9		2.39	4.06	12.0	.277
		13.4		2.73	4.52	11.5	.257
		12.9		3.12	5.08	11.0	.237
		12.3		3.73	5.83	10.5	.217
		11.7		4.49	6.78	9.89	.197
		10.9		5.69	8.10	9.31	.177
		10.0		7.28	9.88	8.64	.157

the real velocity of wind at the level of 10 m U_{10w} is essentially decreased. This effect is considerably enhanced as the wind velocity U_g increases.

4.1.3. The real coefficient of friction C_{10w} is more than twice the background value C_{10t0}, which testifies to the fact that the wave component of momentum flux accordingly exceeds the background (turbulent) component.

4.1.4. For a fixed age of waves, C_{10w} increases with U_{10w} (which is highly veiled by the variability of U_{10w} itself).

4.1.5. As the heaving grows, the value of C_{10w} increases monotonically and rapidly.

4.1.6. For strong waves ($U_g > 20$ m/s), the value of C_{10w} for considerable wave ages ($A > 0.5$) can be sev-

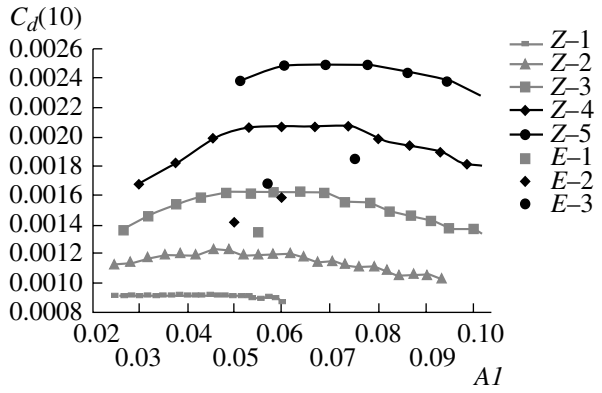

Fig. 1. Dependence of C_{10w} on the wave back age $A1$ and wind velocity U_g (m/s) by Zaslavski's model for spectrum S_{-5}. The model calculations are indicated by lines: (Z–1) $U_g = 5$ ($U_{10} \approx 4.1$); Z–2 – $U_g = 10$ ($U_{10} \approx 7.5$); Z–3 – $U_g = 15$ ($U_{10} \approx 10$); Z–4 – $U_g = 20$ ($U_{10} \approx 13$); Z–5 – $U_g = 25$ ($U_{10} \approx 15$. The experimental data are denoted as large points [15]: (E–1) $U_{10} \approx 10$; (E–2) $U_{10} \approx 12$–13; (E–3) $U_{10} \approx 15$–17.

eral times higher than 0.003, corresponding to extreme observed values [6, 14].

This analysis of Zaslavski's model has quite realistic characteristics, with the exception of the model features indicated in item 5.1.4 (monotonic growth of C_{10w} with A) and 5.1.5 (indicating that the values of C_{10w} are excessively overestimated). Both features contradict empirical data on the decrease in the sea-surface friction as the heaving develops and on the range of scattering of extreme values of C_{10w} [6, 14]. It can be easily seen from the above-described formulas that these features are caused by an overestimated value of $\tilde{\tau}_w$, calculated by formula (38). Furthermore, the calculations show that, for winds with $U_g > 20$ m/s and a wave age of $A \geq 0.5$, formula (39) ceases to work because condition (40) becomes broken.

This problem can be solved through the "adaptation" of the model elements to observational data. For example, this can be achieved by varying both the form of model wave spectrum $S(\omega, \theta)$ and the parametrization type of the increment of the pumping function $\beta(u_*, \omega, \theta)$. In this study, we suppose that the (35)-type representation of function β used by us is reliable due to its reliance upon vast empirical material. Therefore, hereafter, we prefer to vary the form of wave spectrum (30) (see the notes on the spectrum form in Section 3.1).

Based on the above discussion, we performed the same set of calculations of NWBL parameters for the spectrum S_{-5} falling by the law f^{-5}. The corresponding calculations show that, if the trends mentioned in sections 4.1.2–4.1.4 stay unchanged, the model results will not contradict observational data. Graphically, the most important part of the results of these calculations is shown in Fig. 1. It can be seen from Fig. 1 that, in this case, the above-listed "bad" features of the model disappear. This makes it possible to assert that, for the spectrum S_{-5}, Zaslavski's model is highly consistent with the existing generalized observational data [6, 14].

A more detailed comparison between the calculation results and specific experimental data [15] is given below (in Section 4.3), and the shortcomings of this model are described in the final section of the paper.

4.2. The Makin–Kudryavtsev Model [2]

Algorithmically, this model is simpler because its equations do not need to be solved numerically. Here, one merely specifies the wind force on the standard level U_{10} and the form of wave spectrum $S(\omega, \theta)$ and the ANWL parameters are determined by a standard numerical integration technique. This essentially decreases the number of model variables (see the further discussion). At the same time, the calculation time of this model is greater than that of Zaslavski's model, which is caused by the condition that integrals (44) and (45) be calculated with sufficient accuracy.[7]

The results of calculations for the spectrum S_{-4} of the form (30) and for two values of U_{10} are presented in Tables 3 and 4. These results are typical for the MK model. Their features with comments are listed below.

4.2.1. For a fixed wave age A, the values of $C_d(10)$ grow considerably with the wind force U_{10}, which is consistent with experimental data.

4.2.2. $C_d(10)$ grows monotonically with the wave age. However, even extremely large values of the friction coefficient (for fixed calculation parameters described in Section 3.1) are no more than 0.0015. This result does not overlap the range of variations of observed values of $C_d(10)$, which can said to be a defect in the model.

4.2.3. Integral $J(0)$, which, according to (45), corresponds to the parameter $\tilde{\tau}_w$ in (38), exceeds 1 for sufficiently developed waves (see Tables 3 and 4). In view of 2.3.4, which is adopted by the MK model, this situation will not affect the model's efficiency and this feature can be considered one of its advantages. However, physically, supposition 2.3.4 of the model is quite vulnerable because of the need of additional justifications.

A final feature that is characteristic to calculations with Zaslavski's model as well is that the choice of the (30)-type form of spectrum $S(\omega, \theta)$ and our (35)-type representation of the increment of pumping function $\beta(u_*, \omega, \theta)$ are poorly combined. Therefore, the next part of calculations of the friction coefficient by the

[7] In our calculations, the integration error was no more than 1%.

MK model was performed for the S_{-5} spectrum. The results of these calculations are shown in Fig. 2.

It can be seen from Fig. 2 that both the MK and Zaslavski's models are characterized by the emerging tendency of $C_d(10)$ decreasing with the growth of wave age A. This behavior of $C_d(A)$ (common for both models) is caused by the decreased intensity of the spectrum tail with the growth of wave age through the first multiplier $D(A)$ entering into the parametrization of the form of spectrum (30). Here, it is important that, for each of these types of spectra, the dependence of the friction coefficient $C_d(10)$ on the wave age $A1$ in the MK model is similar to that found for Zaslavski's model as well. However, unlike Zaslavski's model, this model makes it possible to also calculate the profile of average wind $U(z)$ up to the viscous layer height $z = z_0^{\nu} \approx 5 \times 10^{-5}$. Leaving a detailed discussion of the MK-model properties to a separate study (a more comprehensive investigation of these aspects of the MK model can be found in [18, 20]), we note that, due to this feature, the MK model is a standard for ADNWL models. Thus, hereafter, this model can be regarded as a basis for constructing an adequate ADNWL model.

At the same time, for the parameters used in the model, the dynamic range of variations of $C_d(10)$ in the MK model is clearly insufficient to comply with observations (a detailed comparison with experimental data will be given below). From the applied point of view, this is the most vulnerable feature of the MK model. A more general analysis of the MK-model feature related to its theoretical postulates is presented in the final section of this paper.

Table 3. Results of calculations with the Makin--Kudryavtsev model for the wind U_g = 10 m/s and spectrum S_{-4}

f_p, Hz	A, 10^{-1}	$A1$, 10^{-2}	$C_d(10)$, 10^{-3}	$J(0)$
.468	3.33	9.48	0.999	.554
.448	3.48	9.13	1.01	.581
.428	3.64	8.77	1.02	.611
.408	3.82	8.41	1.03	.642
.388	4.02	8.05	1.05	.675
.368	4.24	7.69	1.06	.710
.348	4.48	7.32	1.08	.748
.328	4.75	6.95	1.09	.787
.308	5.06	6.57	1.11	.829
.288	5.41	6.19	1.12	.874
.268	5.82	5.81	1.14	.922
.248	6.29	5.42	1.16	.972
.228	6.84	5.02	1.18	1.03
.208	7.49	4.62	1.20	1.09
.188	8.29	4.21	1.22	1.15
.168	9.27	3.80	1.24	1.23
.148	10.5	3.39	1.27	1.31
.128	12.2	2.96	1.30	1.41

4.3. Comparison with Observations

The current state of affairs includes the fact that, in spite of many publications of experimental data, the scientific literature has no such database required for a full-scale verification of the calculation results obtained (for details, see the final section). Particularly, there is a lack (in the necessary amounts) of both synchronous data on two-dimensional wave spectra $S(\omega, \theta)$ in the required frequency range and data on ANWL parameters. In addition, even the most important dependences (for example, the dependence of friction coefficient C_d on wave age $A1$ for different values of U_{10}) have been rarely published and, for this reason, cannot be easily accessed. All of this indicates that there is a need to conduct separate special-purpose measurements (see the final section for a discussion of their character).

However, we can point to a study that includes (albeit poor) data on the empirical values of C_d depending on the back age $A1$ and wind velocity U_{10} [15]. This makes it possible to perform a qualitative preliminary comparison of our calculation results with empirical data of this kind. To this end, let us turn to Figs. 1 and 2. Even a cursory glance over this issue shows that none of the models under consideration is consistent with the experimental data to the required

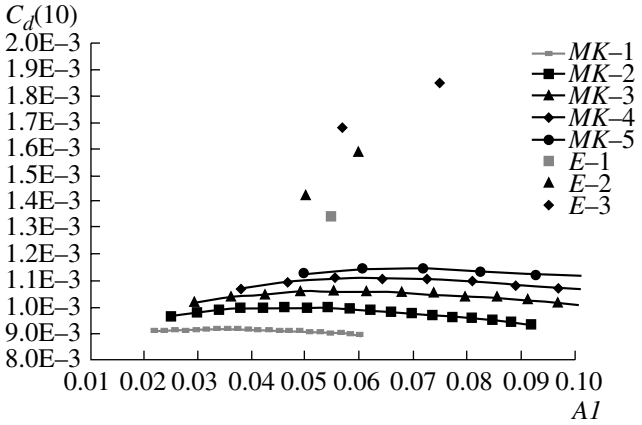

Fig. 2. Dependence of $C_d(10)$ on the wave back age $A1$ and wind velocity U_{10} (m/s) by the Makin–Kudryavtsev model for quickly declining spectra S_{-5}. The model calculations are indicated by lines: (MK–1) U_{10} = 5; (MK–2) U_{10} = 10; (MK–3) U_{10} = 15; (MK–4) U_{10} = 20; and (MK–5) U_{10} = 25. The experimental data are denoted as large points [15]: (E–1) $U_{10} \approx 10$; (E–2) $U_{10} \approx 12$–13; (E–3) $U_{10} \approx 15$–17.

Table 4. Results of calculations with the Makin--Kudryavtsev model for the wind U_g = 20 m/s and spectrum S_{-4}

f_p, Hz	A, 10^{-1}	$A1$, 10^{-2}	$C_d(10)$, 10^{-3}	$J(0)$
.3903	2.00	13.7	.756	.185
.3703	2.11	13.5	.812	.369
.3503	2.23	13.2	.866	.520
.3303	2.36	12.7	.894	.501
.3103	2.52	12.0	.909	.445
.2903	2.69	11.3	.923	.440
.2703	2.89	10.6	.940	.471
.2503	3.12	9.94	.962	.516
.2303	3.39	9.27	.987	.568
.2103	3.71	8.59	1.02	.627
.1903	4.10	7.89	1.05	.693
.1703	4.58	7.19	1.09	.768
.1503	5.19	6.46	1.13	.852
.1303	5.99	5.71	1.17	.946
.1103	7.08	4.94	1.22	1.05
.0903	8.64	4.13	1.28	1.18
.0703	11.1	3.31	1.35	1.36

degree. For example, Zaslavski's model, which covers the whole range of observed values of C_d and, it would seem, reflects the above-mentioned dependences well, actually overestimates the values of the friction coefficient for corresponding winds by almost 1.5 times. It should be taken into account that there is a big difference between the values of the initial geostrophic velocity U_g and the wind U_{10} (see the captions to Fig. 1). Unlike Zaslavski's model, the MK model yields an essential (from 30 to 60%) underestimation of calculated values of C_d when compared to observational data on the friction coefficient in this experiment.

In this case, quantitative data on the form of spectrum $S(\omega, \theta)$ are unavailable to us. Therefore, the actual deviations of the results of these calculations from observed values cannot be estimated. It cannot be excluded that using the exact quantitative data of $S(\omega, \theta)$ will improve the comparison results. However, the results of these comparisons already make it possible to conclude that the MK and Zaslavski's models are unsatisfactorily consistent with experimental data (at least, as they are given in the literature mentioned above). In view of the strong features of these models, their modification can be assumed to be able to essentially improve the situation. It is this goal that is expected to be achieved by the analysis given below.

5. CONCLUDING REMARKS

Let us make conclusions about the shortcomings and advantages of the above-described ADNWL models aimed at searching for ways to improve the degree of their reliability and adequacy to observations.

5.1. Zaslavski's Model

The advantages of this model can be listed as follows: (1) quick computational performance; (2) a number of empirical laws can be adequately described; and (3) essential theoretical validity, including the possibility of using atmospheric stratification.

The shortcomings of the model are: (1) the use of planetary-scale parameters (geostrophic wind and Coriolis parameter), (2) the dependence of the solution on local latitude, (3) postulating the wind profile $U(z)$ and excluding its calculation in the layer of wave fluctuations of velocity, (4) high sensitivity to the choice of the law of the spectral tail fall-off, and (5) the overestimated model values of $C_d(U_{10}, A1)$.

This model can be improved through its modification, including the elimination of the above-mentioned shortcomings (first of all, (1) and (2)). It seems that the theoretical approach to the problem on the basis of the fundamental study by Kazanski and Monin [13]

5.2. The Makin–Kudryavtsev Model

This model has the following benefits: (1) one can calculate the wind profile up to the level of the viscous sublayer (the theoretical and practical importance of this feature was discussed in [18]), (2) the model operation is stable and its results for a wide range of forms of wave spectra have reasonable orders of magnitude, and (3) the physical validation of the model is substantial.

The defects in this model are: (1) the calculated friction coefficient has a small dynamical variation range, (2) postulate 2.3.4 (see Section 2.3) of the model is insufficiently justified, (3) the calculation interval is prolonged (compared to Zaslavski's model), and (4) atmospheric stratification is not taken into account.

It should be noted that, generally, the problems with the MK model are a continuation of its benefits. Indeed, it is item 2.3.4 that is responsible for benefits (1) and (2) indicated above, while benefit (1) leads to defect (3). Therefore, the MK model can be improved by adjusting the parametrization of the increment of pumping function $\beta(u_*, \omega, \theta)$ and (related to that) justifying item 2.3.4 of the model more thoroughly.

The latter, together with the problem of constructing an adequate parametrization of the tail of wave

spectrum $S(\omega, \theta)$, constitute the list of general problems for the construction of any of the ADNWL models. Now, let us discuss these problems.

5.3. Parametrization of the Increment of Pumping Function

Currently, the possibilities that the form of $\beta(u_*, \omega, \theta)$ can be empirically determined seem to be considerably exhausted. This is caused by both the difficulties in the direct measurement of the growth rate of wave components at time scales of some tens or hundreds of wave periods (it is here that the wave spectrum is defined) and the lack of diversity in the existing measurement techniques.[8] Indeed, at the above-mentioned timescales, the energy (and momentum) transfer from wind to wave components is simultaneously accompanied by an intensive nonlinear transfer between the components (especially in the high-frequency range) and a very complex (in the physical sense) process of wave-component dissipation. Here, both of these processes are almost immeasurable and can merely be calculated numerically by some accepted models. It is only this binding that makes the more or less reliable measurements of $\beta(u_*, \omega, \theta)$ real, even (as is easily understandable) in a quite limited frequency range. In spite of this, one can still expect some progress in this direction given the modern-day level of technology (see, for example, [21]).

In addition, one should not ignore that it is possible to construct a semi-empirical model function $\beta(u_*, \omega, \theta)$ through a correction of a (35)-type formula, ensuring that it can be used for solving the problem of ADNWL model construction. In this relation, both numerical calculations and very distinct reliable observations and measurements of heaving and ANWL characteristics may be useful.

The second method for correcting the form of $\beta(u_*, \omega, \theta)$ lies in the field of methods for numerically modeling the air–water interface as a whole. Here, there are certain successes based on the numerical solution of the system of exact equations of hydrodynamics in curvilinear coordinates for both the ANWL and a rough-sea surface.[9] The problem with this approach is in the choice of a sufficient number of Fourier-expansion components that are required for taking into account and describing the spectral composition of the nonstationary field of waves in a wide frequency range. With a specific art of numerical modeling and corresponding computing hardware, one can expect considerable progress in solving this problem; however, only the stage of breakdowns is considered. In addition, special care must be taken to exclude the influence of mechanisms of nonlinear energy transfer by spectrum (small periods of the calculated evolution, small intensity of heaving, etc.) on the wave dynamics. For practical needs, one can generalize these kinds of numerical results by their approximate extrapolation to real waves that are far from numerical idealizations. However, private reports (known by the author) on the existing results in the field of numerical modeling of the interface dynamics and the rate of their consistency with empirical data make it possible to expect some possible progress in solving this problem.[10]

5.4. Parametrization of the Wave-Spectrum Tail

Unlike the above, this is a purely technical matter: the solution to this problem is completely controlled by the technical setup of relevant observations. In view of this, it will be interesting to set the requirements that should be met by the conditions of required observations.

First, the experimental equipment must be able to reconstruct the two-dimensional energy wave spectrum $S(\omega, \theta)$ in the widest range from 0.1 to 10–15 Hz (the requirements to the angular ranges are less significant). Taking into account the experimentally revealed strong frequency dependence of the wave spectrum on frequency [3, 4], it can be naturally expected that the corresponding equipment includes a set of meters of both contact and remote types. The first type of instruments reconstructs the energy-carrier part of the spectrum, which is then "spiced" with measurements of the high-frequency part of heaving up to the capillary range (the measurement of which can be performed more easily by the remote measurement method). Modern-day technology has such meters, which extends the possibilities of experimenters. It should be noted that this spicing of gravitational and gravitational–capillary ranges needs to be performed within one and the same series of measurements to essentially improve the already known (so-called "model") representations for the form of $S(\omega, \theta)$ constructed behindhand by a formal coupling of measurements conducted by different authors (and obtained at different times at that), as often has been the case (see, for example, [2, 12, 22, 23]).

Second, the measurements under consideration imply that they are carefully planned and systematic. This means that the heaving measurements must be performed repeatedly at well-controlled (desirably, close to ideal conditions in terms of the constancy in the wind force and direction) meteorological conditions during quasi-stationary periods (15–20 min) and, most importantly, for different winds and wave

[8] A view of the difficulties and diversity of accompanying problems can be obtained, for example, from recent works [15, 21].

[9] : Part of the huge bibliography on this matter can be found in [5].

[10] We are referring to reports by D.V. Chalikov and Yu.I. Troitskaya in a meeting within the Russian Foundation for Basic Research (RFBR), project no. 07-05-12011_ofi.

ages. When these conditions are satisfied and the measurements are complex, one can adequately parameterize the form of $S(\omega, \theta)$, depending on wave-formation conditions, without any principal difficulties.

Third, one must synchronize the measurements of the two-dimensional spectra of heaving and the full set of ANWL characteristics. Here, a problem arises concerning the measurement of the average wind profile $U(z)$ and the flux profile $\tau(z)$ up to the mean-surface level resolution height, which is on the order of fractions of a centimeter.[11] To our knowledge, there have been no examples of such measurements. However, it can be formally supposed that such measurements can be performed based on the methods of optical sounding (optovelosymmetry [24]). In view of the extreme difficulty in performing such measurements, one can presumably accept that, at the current technological level, measuring profiles $\tau(z)$ and $U(z)$ from the height of the standard level to the height crests of maximum waves (synchronously with the wave-spectra measurements) is rather realistic. Such data would be quite sufficient to construct an experimental basis, allowing the ADNWL model to be checked for reliability.

Based on literature data, it can be supposed that such measurements have already been widely used abroad [15]. This means that, in the near future, they will be implemented in our country too. The communicational and organizational problem is to ensure that such data, in the same way as the above-mentioned calculation results, become available to a wide circle of researchers. Then it will be possible both to perform a comprehensive verification of versions of ADNWL models and to construct the final and most adequate version of that model.

5.5. Notes on Model Testing by Authors

In conclusion, we can say a few words about the results of testing the above-mentioned theories performed by the model authors themselves [7, 12, 22, 23]. In each of these test cases, in the same way as in the present work, the particular form of wave spectra is overly schematic and the increment functions $\beta(u_*, \omega, \theta)$ are approximated very conditionally. Naturally, in the narrow field of partial wave-formation cases considered by the authors of the models, one can see a reasonable consistency between the observed and calculated data. However, as is shown by the above-described detailed calculations, improving ADNWL models has been far from being completed. The same thing is testified to by the ongoing series of studies by Kudryavtsev and Makin [2, 22, 23] and by many other works aimed at solving the problem of improving the adequacy of ADNWL models.

It clearly follows from here that both the theoretical and observational databases need to be further developed in various aspects, the most important of which were mentioned by us.

[11] From the theoretical point of view, it is the profile $U(z)$ at such small heights and especially in the area from the wave-ground level to the average wave-crest level that is of highest interest.

ACKNOWLEDGMENTS

This study was supported by the Russian Foundation for Basic Research, project no. 07-05-12011-ofi. The author is grateful to the participants of seminars related to this project and to the reviewer for a number of useful comments.

REFERENCES

1. M. M. Zaslavskii, "On Parametrical Description of the Atmospheric Surface Layer," Izv. Akad. Nauk, Fiz. Atmos. Okeana **31** (5), 607–615 (1995).
2. V. K. Makin and V. N. Kudryavtsev, "Coupled Sea Surface-Atmosphere Model. Pt.1 Wind over Waves Coupling," J. Geophys. Res. **104** (C4), 7613–7623 (1999).
3. M. A. Donelan, J. Hamilton, and W. H. Hui, "Directional Spectra of Wind Generated Waves," Phil. Trans. R. Soc. London **A315** 509–562 (1992).
4. O. M. Fillips, *Dynamics of the Upper Oceanic Layer* (Gidrometeoizdat, Leningrad, 1980) [in Russian].
5. Yu. I. Troitskaya and G. V. Rybushkina, *Quasilinear Model of Interaction of Surface Waves with Strong and Hurricane Winds*, Preprint No. 755 (Inst. Prikl. Fiz. Ros. Akad. Nauk, Novgorod, 2008) [in Russian].
6. M. A. Donelan, et al., "On the Dependence of Sea Surface Roughness on Wave Development," J. Phys. Oceanorg **23**, 2143–2149 (1993).
7. M. M. Zaslavskii and A. V. Glazunov, "On Different Approaches to the Atmospheric Surface Layer Parametrization," Izv. Akad. Nauk, Fiz. Atmos. Okeana **34** (4), 508–516 (1999).
8. A. S. Monin and A. Ya. Yaglom, *Statistical Hydrodynamics* (Nauka, Moscow, 1965), Part 1 [in Russian].
9. D. V. Chalikov, "The Parameterization of the Wave Boundary Layer," J. Physical Oceanogr. **25** (6), 1333–1349 (1995).
10. P. E. A. M. Janssen, "Quasi-Liner Theory of Wind Wave Generation Applied to Wind Wave Forecasting," J. Phys. Oceanogr. **21**, 1389–1405 (1991).
11. J. W. Miles, "On the Generation of Surface Waves by Shear Flows. Pt. 1," J. High Resolut. Chromatogr. Chromatogr. Commun. **3** (2), 185–204 (1957).
12. M. M. Zaslavskii, M. B. Zalesnyi, I. M. Kabatchenko, et al., "On the Self-Adjusted Description of the Atmospheric Boundary Layer, Wind Waves, and Sea Currents," Okeanologiya **46** (2), 178–188 (2006) [Oceanology **46** (2), 159–169 (2006)].
13. A. B. Kazanskii and A. S. Monin, "On the Dynamic Interaction between the Atmosphere and Earth Surface," Izv. Akad. Nauk SSSR, Ser. Geofiz., No. 5, 786–788 (1961).

14. W. M. Drennan, K. K. Kahma, and M. A. Donelan, "On Momentum Flux and Velocity Spectra over Waves," Boundary-Layer Meteorol., 1993, vol. 63, pp. 65–96. **92**, 489–515 (1999).
1 15. W. M. Drennan, H. C. Graber, D. Hauser, et al., "On the Wave Age Dependence of Wind Stress over Pure Wind Seas," J. Geophys. Res. **108** (C3), 8062–8075 (2003).
16. T. B. Elfouhaily, B. Chapron, K. Katsaros, et al., "A Unified Directional Spectrum for Long and Short Wind-Driven Waves," J. Geophys. Res. **107** (1997).
17. L. Yan, *An Improved Wind Input Source Term for Third Generation Ocean Wave Modelling. Scientific Report WR-87-8* (KNML, The Netherlands, 1987).
2 18. Yu. A. Volkov, V. G. Polnikov, and F. A. Pogarskii, "On the Wind Profile near a Wavy Surface," Izv. Akad. Nauk, Fiz. Atmos. Okeana **43** (2), 279–288 (2007) [Izv., Atmos. Ocean. Phys. **43** (2), 250–258 (2007)].
19. S. S. Zilitinkevich and I. N. Esau, "Resistance and Heat Transfer Laws for Stable and Neutral Planetary Boundary Layers: Old Theory Advanced and Re-Evaluated," Q. J. R. Meteorol. Soc. **131**, 1863–1892 (2005).
20. V. G. Polnikov, Yu. A. Volkov, and F. A. Pogarskii, 2 "Interpretation of Variations in the Characteristics of the Boundary Layer with a Numerical Model," Izv. Akad. Nauk, Fiz. Atmos. Okeana **39** (3), 410–421 (2003) [Izv., Atmos. Ocean. Phys. **39** (3), 369–379 (2003)].
21. V. Yu. Karaev and G. N. Balandina, "Modified State Spectrum and Remote Probing of the Ocean," Issled. Zemli Kosmosa, No. 5, 45–56 (2000).
22. V. N. Kudryavtsev and V. K. Makin, "Coupled Sea Surface–Atmospheric Model Pt. 2," J. Geophys. Res. **104** (4), 7625–7639 (1999).
23. V. N. Kudryavtsev and V. K. Makin, "The Impact of Air Flow Separation on the Drag of the Sea Surface," Bound. Layer Meteorol. **98**, 155–171 (2001).
24. M. A. Donelan, B. K. Haus, N. Reul, et al., "On the Limiting Aerodynamic Roughness of the Ocean in Very Strong Winds," Geophys. Res. Lett. **31**, L18306 (2004).

SPELL: 1. Hauser, 2. Pogarskii